

Supporting Information

Antimony alloying electrode for high-performance sodium removal: how to use a battery material not stable in aqueous media for saline water remediation

Stefanie Arnold,^{1,2} Lei Wang,^{1,2} Öznil Budak,^{1,2}

Mesut Aslan,¹ Pattarachai Srimuk,¹ Volker Presser^{1,2,*}

¹ INM - Leibniz Institute for New Materials, 66123 Saarbrücken, Germany

² Department of Materials Science and Engineering, Saarland University, 66123 Saarbrücken, Germany

* Corresponding author's E-Mail: volker.presser@leibniz-inm.de

Supporting Table

Table S1: Results of the elemental analysis (CHNS/O).

	CHNS/O elemental analysis (mass%)				
	Carbon	Hydrogen	Nitrogen	Sulfur	Oxygen
Antimony powder	0.18±0.11	Not detected			5.66±0.04

Supporting Material Characterization

We used a co-precipitation method to obtain the antimony nanopowder. Scanning electron micrographs, X-ray diffraction data, and Raman data are given in **Figure S1**. **Figure S1A**, the scanning electron micrograph shows partially agglomerated particles with a primary size of about 10-40 nm. The X-ray diffractogram (**Figure S1C**) is consistent with elemental antimony (space group of $R\bar{3}m$, ICSD: #55402, $a=4.307$ Å). Rietveld analysis yields an Sb phase content of about 97-98 mass% with a small amount of Sb_2O_3 . This aligns with the small amount of oxygen found from chemical CHNS/O elemental analysis (*Supporting Information, Table S1*). The Raman spectra of antimony at ambient conditions (**Figure S1D**) shows two peaks at 113 cm^{-1} and 150 cm^{-1} , which agrees with previous works on antimony.¹⁻³ Trigonal antimony forms stacked layers of atoms along the hexagonal axis. This structure results in two Raman active modes, the A_{1g} mode at 150 cm^{-1} and a two-fold degenerated E_g mode at 115 cm^{-1} , whereby the A_{1g} mode corresponds to the longitudinal motion of the atom planes and the E_g mode the transverse motion.² The Raman spectra also shows the presence of small amounts of Sb_2O_3 from the broad and low-intensity peak at around 270 cm^{-1} (Sb-O-Sb). The antimony oxide is most likely present in the form of thin skin around the antimony particles, which would act as an insulative layer between the antimony particle. This would result in high resistance of the electrode and poor electrochemical performance with a capacity close to zero. Therefore, the use (and choice) of the conductive additive plays a central role.

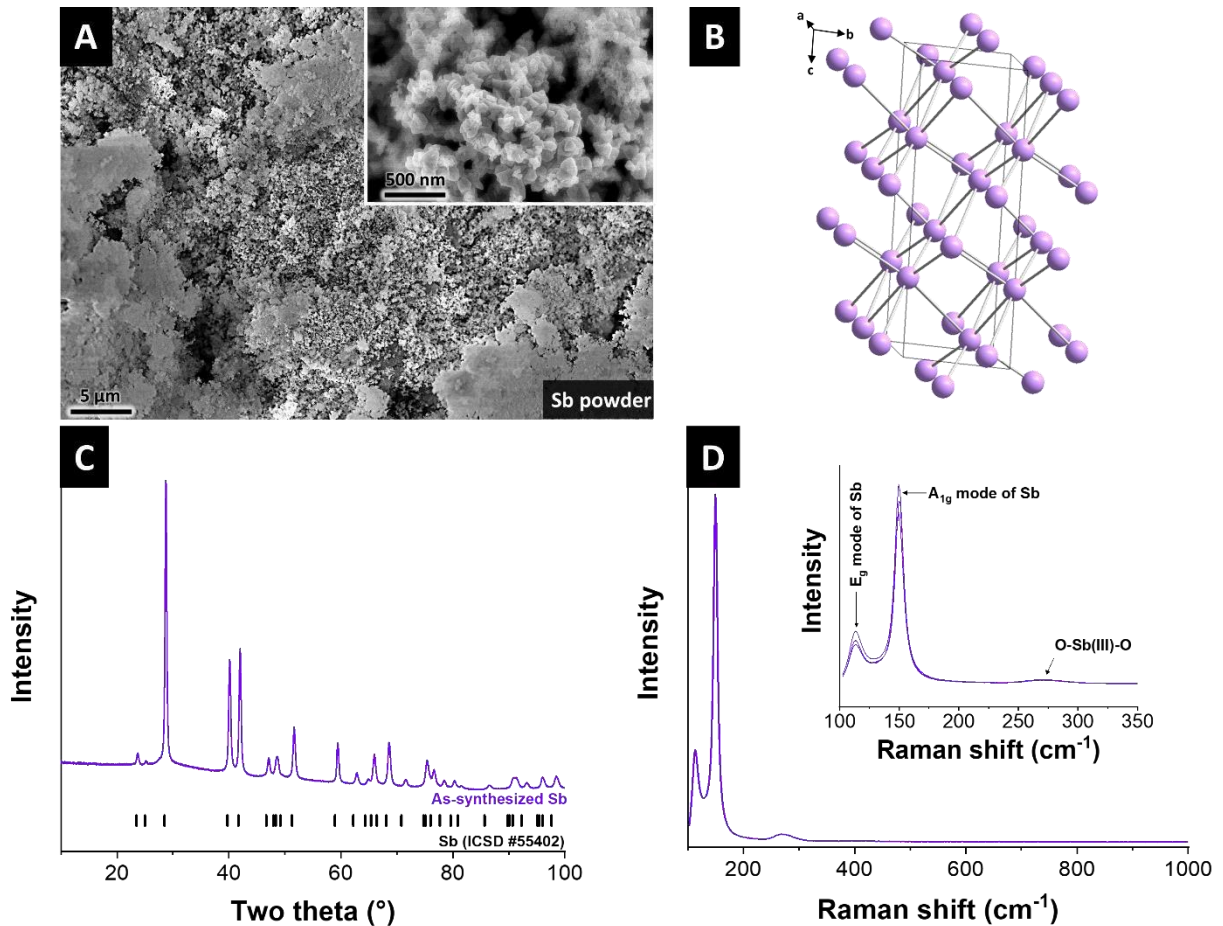


Figure S1: Material characterization of the as-synthesized antimony. (A) Scanning electron micrographs. (B) Crystal structure. (C) X-ray diffraction pattern. (D) Raman spectra (the inset shows the Raman mode assignment and three characteristic individual spectra).

We also analyzed the ceramic NASICON membrane. The XRD pattern in **Figure S2A** shows the characteristic peaks of low-NASICON (powder diffraction file, PDF 84-1184, space group C2/c; $a=15.674 \text{ \AA}$). Rietveld analysis yields a NASICON phase content of about 97-98%. There is also a second phase present, namely 2-3 mass% baddeleyite-type ZrO₂ (PDF 89-9066). The presence of ZrO₂ can potentially be due to both unreacted precursor and abrasion of the grinding balls.

The sintered material exhibits a theoretical density of 78%. This means the material still has open pores which are accessible to the electrolyte. For this reason, the pores are sealed by a post epoxy infiltration to close the pores of the membrane. The tightness of epoxy filled membranes was provided by checking the water uptake to be <1 mass%. Membranes with a diameter of 4 cm and a thickness of 300 μm were prepared for use as a membrane between the organic and the aqueous side in the desalination cell.

Photographs of the NASICON discs with a thickness of 950 μm for electrochemical testing and NASICON discs with a thickness of 300 μm for desalination testing are shown in **Figure S2B**. For the electrochemical testing of the NASICON electrode, both sides of the electrode were sputtered with platinum. **Figure S2C-D** shows scanning electron micrographs of NASICON powder and NASICON membrane. The ceramic matrix is composed of sub-micrometer particles, and the interparticle pore space in the NASICON membrane is effectively filled with epoxy resin.

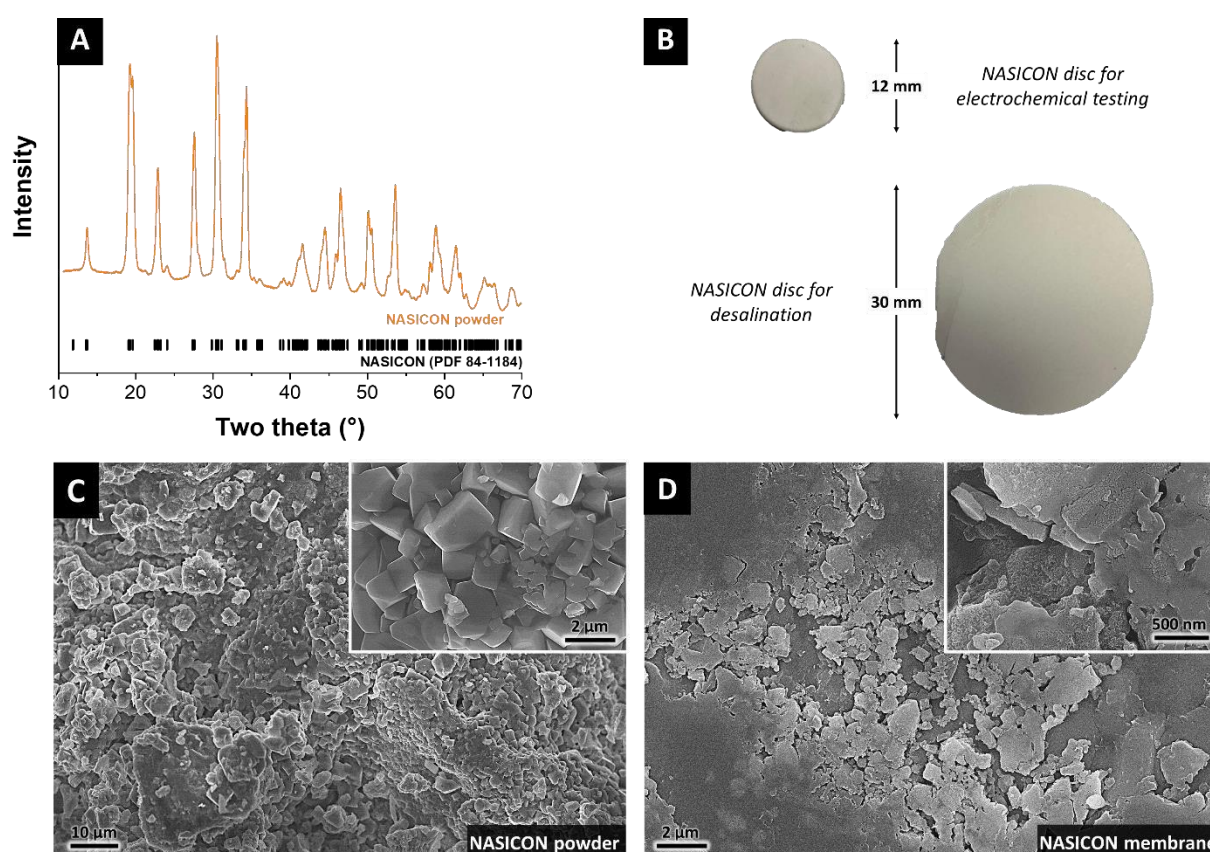


Figure S2: Material characterization of NASICON. (A) Diffractogram of the final NASICON powder, (B) photograph of NASICON discs for electrochemical characterization and desalination. (C) scanning electron micrographs of NASICON powder. (D) scanning electron micrographs of epoxy infiltrated NASICON membrane.

Supporting Electrochemical Characterization

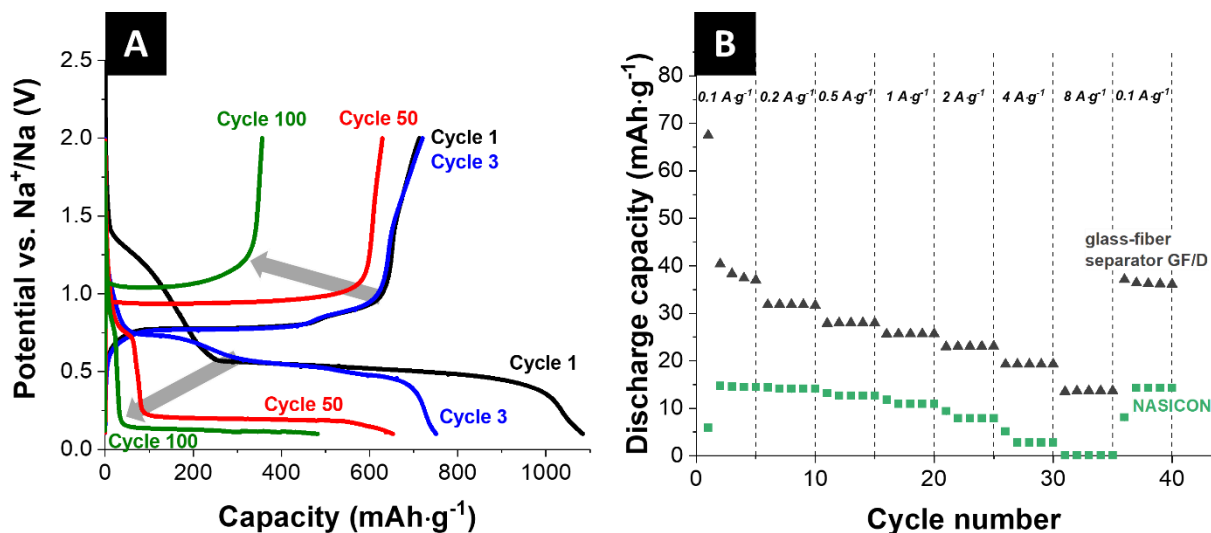


Figure S3: (A) Galvanostatic charge and discharge profiles of Sb/C electrode of the 1st, 3rd, 50th and 100th cycle at 200 mA·g⁻¹ between 0.1 V and 2.0 V vs. Na⁺. (B) Rate performance of the activated carbon cloth full-cell from galvanostatic charge/discharge cycling at different specific currents.

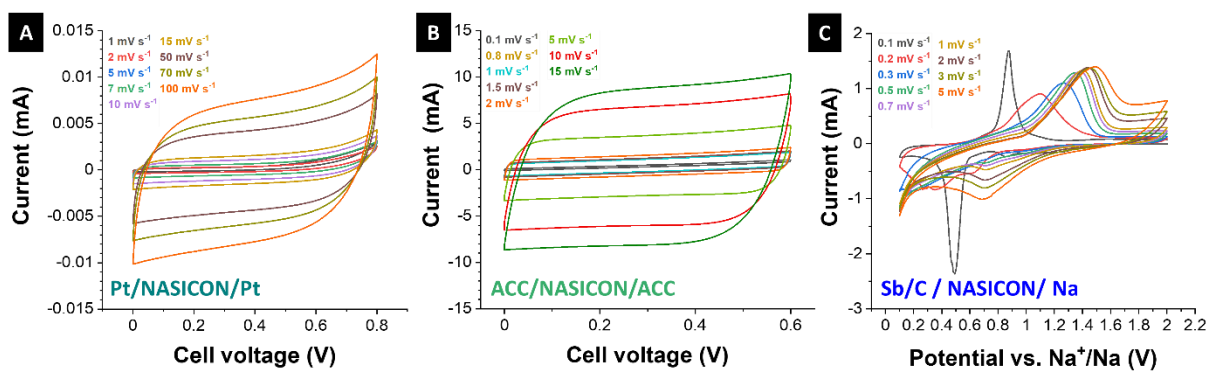


Figure S4: Cyclic voltammograms at different scan rates of (A) just the NASICON membrane contacted with platinum, (B) two activated carbon cloth electrodes separated by the NASICON membrane, and (C) Sb/C vs. Na separated by the NASICON membrane.

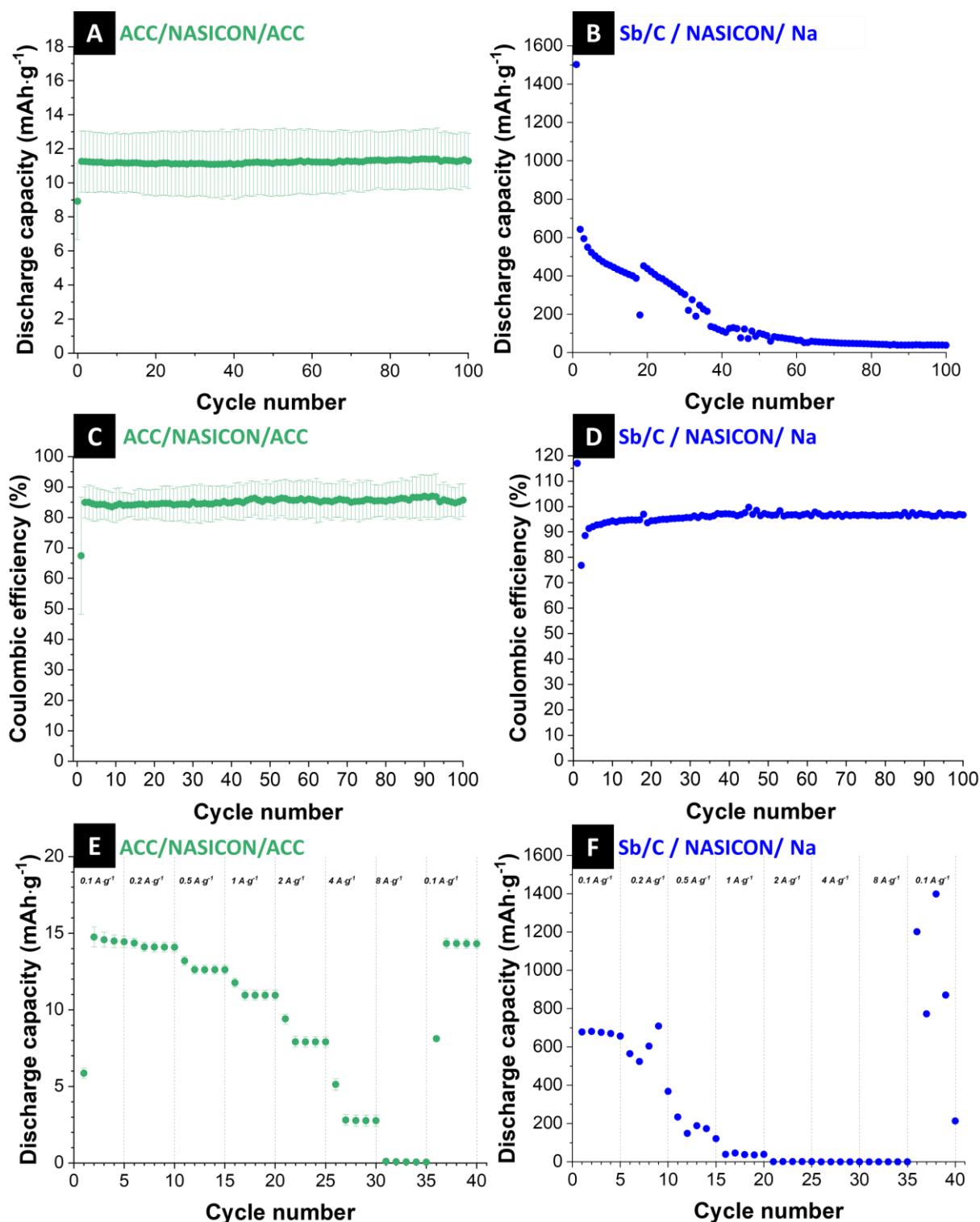


Figure S5: Electrochemical performance with NASICON as separator. (A) Electrochemical cycling stability at specific current of 200 mA g⁻¹ of activated carbon cloth full-cell with NASICON membrane. (B) Electrochemical cycling stability at specific current of 200 mA g⁻¹ of Sb/C vs. Na. (C) Coulombic efficiency at charging/discharging rates of the activated carbon cloth full-cell. (D) Coulombic efficiency of Sb/C electrode. (E) Rate performance of the activated carbon cloth full-cell from galvanostatic charge/discharge cycling at different specific currents. (F) Rate performance of the Sb/C electrode from galvanostatic charge/discharge cycling at different specific currents between 0.1-2.0 V vs. Na/Na⁺.

Supporting References

1. A. Roy, M. Komatsu, K. Matsuishi and S. Onari, *Journal of Physics and Chemistry of Solids*, 1997, **58**, 741-747.
2. O. Degtyareva, V. V. Struzhkin and R. J. Hemley, *Solid State Communications*, 2007, **141**, 164-167.
3. M. L. Bansal and A. P. Roy, *Physical Review B*, 1986, **33**, 1526-1528.